Applied Thermal Engineering 50 (2013) 837–847

Contents lists available at SciVerse ScienceDirect

Applied Thermal Engineering

journal homepage: www.elsevier.com/locate/apthermeng

Effective heating for tumors with thermally significant blood vessels during hyperthermia treatment

Huang-Wen Huang [a], Chihng-Tsung Liauh [b], Tzyy-Leng Horng [c], Tzu-Ching Shih [d], Chi-Feng Chiang [e], Win-Li Lin [e,f,*]

[a] Department of Innovative Information and Technology, Langyang Campus, Tamkang University, I-lan, Taiwan
[b] Department of Mechanical Engineering, Kun-Shan University, Tainan, Taiwan
[c] Department of Applied Mathematics, Feng Chia University, Taichung, Taiwan
[d] Department of Biomedical Imaging and Radiological Science, China Medical University, Taichung, Taiwan
[e] Institute of Biomedical Engineering, College of Medicine and College of Engineering, National Taiwan University, No. 1, Sec. 1, Jen-Ai Road, Taipei, Taiwan
[f] Division of Biomedical Engineering, National Health Research Institutes, Miaoli, Taiwan

HIGHLIGHTS

- Cooling effects by blood flow during hyperthermia treatments could be improved.
- The preheating strategy places zone on the blood vessel next to treated tumor region.
- Higher preheating zone temperature and longer preheating zone length are helpful.
- The preheating could prevent extreme required power deposition in the tumor region.
- We proposed the preheating strategy using a single blood vessel and vascular model.

ARTICLE INFO

Article history:
Received 29 March 2012
Accepted 17 July 2012
Available online 25 July 2012

Keywords:
Thermally significant blood vessels
Cooling effect
Hyperthermia
Adaptive optimization
Preheating zone
Absorbed power deposition

ABSTRACT

Significant cooling effect by blood vessels, particularly in treated tumor region, during hyperthermia treatment has been recognized by researchers. The present study investigated a heating strategy, using a preheating zone and adaptive optimization, to effectively reduce the cooling effect as thermally significant blood vessels flowed through treated region during hyperthermia treatment. The preheating zone is located in a vessel's entrance region adjacent to treated tumor and the heating strategy attempted to elevate blood temperature before blood flowing into the treated region. We numerically calculated blood and tissue temperatures using 3-D models and the goal of treatment was to reach a uniform therapeutic temperature in the tumor region using the proposed heating strategy. Results showed first, for large blood vessels, the heating strategy effectively elevated blood temperature at the entrance of treated tumor and reduced total tumor power deposition. Consequently, it helped to reach the ideal treated temperature on tumor more effectively, and avoided extreme power deposition due to the cooling effect of blood vessels entering the treated region. For small blood vessels, the preheating zone could further improve the treatment result. Secondly, heating flowing blood with adaptive optimization results in a unique phenomenon along blood flow paths. That is a strong convective nature of blood flow, which creates high thermal gradients in the treated region. Thus, it plays a different and significant role in adaptive optimization process as compared to thermal diffusion of solid tissues.

1. Introduction

Reaching uniform target temperature in the treated region is the desirable goal of tumor hyperthermia. However, complicated biological vasculature inside human body made the treatment hard to reach this kind of temperature distribution [1,2]. Thus, to

* Corresponding author. Institute of Biomedical Engineering, College of Medicine and College of Engineering, National Taiwan University, No. 1, Sec. 1, Jen-Ai Road, Taipei, Taiwan. Tel.: +886 2 2312 3456x81445; fax: +886 2 2394 0049.
E-mail address: winli@ntu.edu.tw (W.-L. Lin).

1359-4311/$ – see front matter © 2012 Elsevier Ltd. All rights reserved.
http://dx.doi.org/10.1016/j.applthermaleng.2012.07.018

Nomenclature

c	specific heat capacity, J kg^{-1} °C^{-1}
CV	convergence value
D	diameter of blood vessel, mm
H	length of control volume in z direction, cm
k	thermal conductivity, W m^{-1} °C^{-1}
L	length of control volume in x direction, cm
L_{pre}	the preheating zone length, mm
m	mass flow rate, kg s^{-1}
n	the iteration number
Nu	Nusselt number of blood vessels
P	absorbed power deposition, W m^{-3}
R	radius of blood vessel, mm
T	temperature, °C
$\dot{w}$	perfusion rate, kg m^{-3} s^{-1}
W	length of control volume in y direction, cm
x	coordinate in the x direction
y	coordinate in the y direction
z	coordinate in the z direction
ΔC_n	cost function increment at nth iteration
ΔT	temperature difference, °C

Greek symbols

π	mathematical constant
ρ	density, kg m^{-3}

Subscripts

pre	preheating zone
b	blood
bv	blood vessel
i	index of node number; index of level number of blood vessels
ideal	ideal temperature in the treated tumor or desired temperature in the preheating zone
n	iteration
s	absorbed source power
w	vessel wall

reach the goal requires precise absorbed power deposition with optimization during treatment. Recently Huang et al. [3] presented a 3-D vascular model with optimization to treat the specific interior tumor. The paper addressed significant cooling effect by large blood vessels at the entrance to the treated region, particularly for those vessels flowing into the region. Historically, the cooling effect generated by thermally significant blood vessels has been investigated by many researchers. At first, blood could carry heat out and mix with warmer tissue temperatures and Pennes [4] studied the cooling effect by proposing a blood perfusion term in the mathematical formulation. Pennes equation is an approximation to the temperature field without considering impact of large blood vessels. Chen and Holmes [5] investigated micro-vascular contributions in tissue heat transfer. They presented important properties of vascular compartments which described vascular thermal impact in their bio-heat equation. In 1980, Chato [6] investigated heat transfer of blood vessels and indicated that large arteries have significant impact on the temperature distribution of surrounding tissue. Continued from Chato's work, during 1990s, Huang [7] used a 3-D tissue and blood vessel model to numerically investigate the impacts of large blood vessels on hyperthermia cancer treatments, and Huang et al. [8] developed analytical solutions of Pennes bio-heat transfer equation with a blood vessel by neglecting axial conduction effect. Baish [9] presented heat transport by countercurrent blood vessels in the living tissues. Crezee and Lagendijk [10,11] experimentally verified temperature profiles around large artificial vessels in the perfused tissues.

Rawnsley et al. [12] illustrated the experimental blood temperature data measured in the thighs of anesthetized greyhound dogs under hyperthermic conditions heated by scanned focused ultrasound. Furthermore, Kolios et al. [13] presented ultrasonic lesion formation in rat liver with short ultrasound exposure time, approximately 8 s, which showed that blood flow played an important role in the thermal dose distribution. Lin et al. [14] used external ultrasound power and optimization to treat a cubic tumor region. Tharp and Roemer [15] showed an optimized power deposition with finer resolution during hyperthermia treatment. However, they did not consider the impact of blood flow in the treated region. Huang et al. [3] investigated optimized temperature and absorbed power density distributions using vascular model involving blood flows.

The concept of preheating blood has been raised by Crezee and Lagendijk [11,16], and Roemer [17]. They suggested preheating the large vessels before they enter the heated volume as a solution to the cooling effect of large vessels. In this study, we proposed a heating strategy to optimally realize the idea.

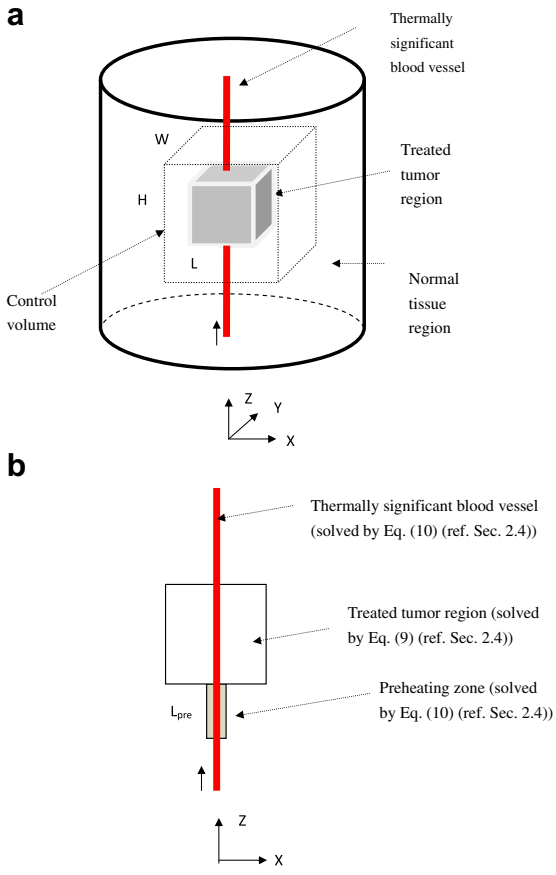

Fig. 1. (a) Shows the geometric model illustrating a thermally significant blood vessel passing through a treated tumor region at the center with blood flowing upward. (b) A projection view on X–Z plane of Fig. 1(a) indicates a preheating zone with length (L_{pre}) and temperature (T_{pre}) on a thermally significant blood vessel.

Table 1
Significant vessel diameters and average flow rates from Kolios et al. [13].

Blood vessel diameter (mm)	Average velocity (cm/s)
1.4	10.5
1.0	8.0
0.8	7.5
0.6	6.0
0.4	5.5
0.2	3.4

2. Methods

2.1. Formulation of the problem

To present our studies, we simplified the problem and used a thermally significant blood vessel passing through a treated tumor region at the center. The tumor is a volume of 1 cm cube. The domain of control volume in the study is 4-cm (H) by 4-cm (W) by 4-cm (L), for it is sufficiently large to describe the temperature distributions around tumor and requires less computational time. A geometric model illustrating this situation is shown in Fig. 1(a) with blood flowing upward in the current study.

To raise the blood temperature before it enters the treated region, the preheating zone is located at the entrance as illustrated in Fig. 1(b), a projection view on x–z plane of Fig. 1(a). The preheating zone was located at the vessel entrance region, adjacent to treated tumor, with preheating length (L_{pre}) and desired preheating temperature (T_{pre}). The cross section area of preheating zone was chosen as 1-mm by 1-mm. Thus, the zone could completely cover and heat blood within the blood vessel as well as some normal tissue area. The information about the significant blood vessel sizes and average mass flow rates, which is shown in Table 1, is based on Kolios' report [13].

2.2. Adaptive optimization scheme

An adaptive optimization process was employed in the treated tumor region during hyperthermia treatment. The scheme was

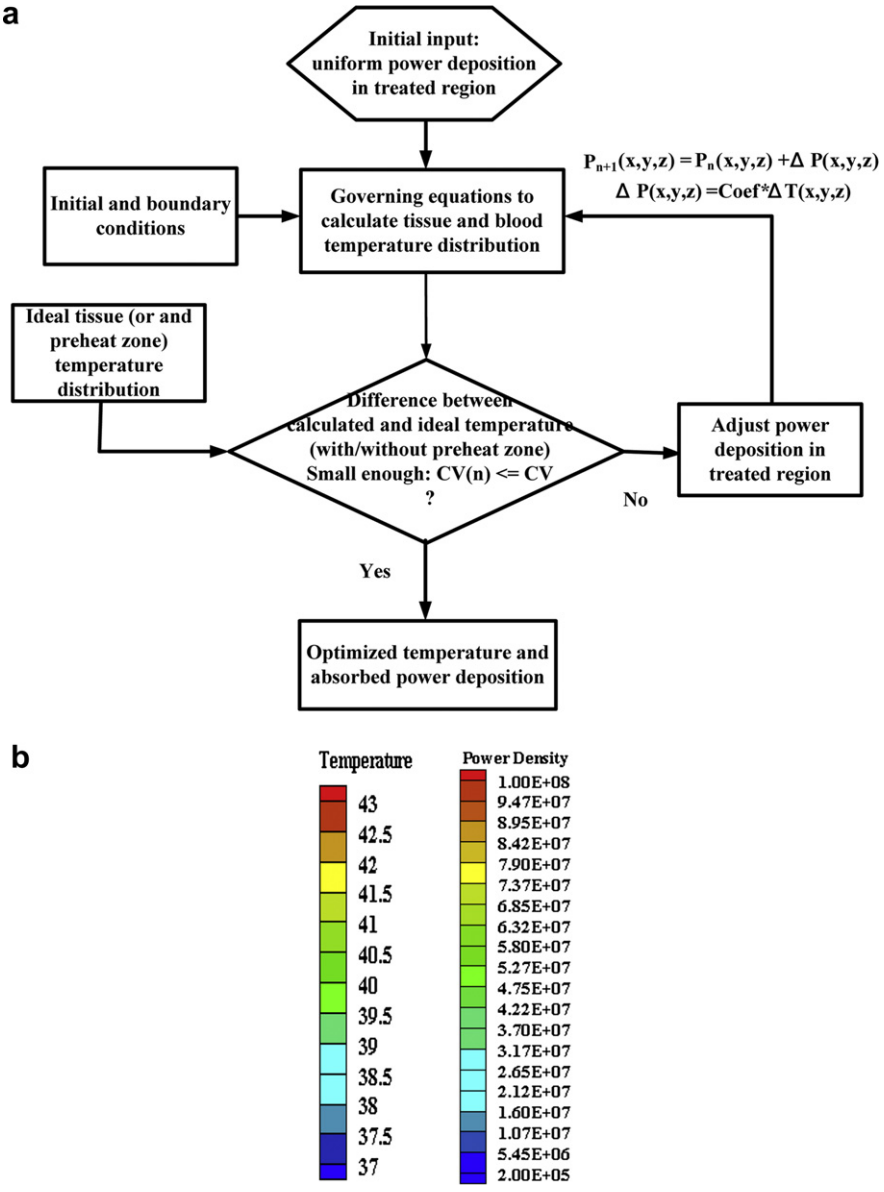

Fig. 2. (a) The flow chart of adaptive optimization scheme (a finer resolution) to reach an ideal temperature in the treated region. The desired preheating temperature (T_{pre}) is in the range of 40–42 °C (b) the legends of temperature and power density deposition in 2-D plots throughout the paper. (unit in legends, Temperature: °C and Power Density: W m^{-3})

identical to the one published by Huang et al. [3] with a variant. That is to include the optimization of desired preheating zone temperature in the scheme. Adaptive absorbed power density scheme is,

$$P_{n+1}(x,y,z) = P_n(x,y,z) + \Delta P(x,y,z) \quad (1)$$

$$\text{where } \Delta P(x,y,z) = \text{Coef}^*\Delta T(x,y,z) \quad (2)$$

$$\text{and } \Delta T(x,y,z) = T_{\text{ideal}} - T(x,y,z) \quad (3)$$

where P is absorbed power density (W m^{-3}), which is a function of space; Coef is 10,000 here, n is the iteration number and ΔT is the difference between ideal temperature and calculated temperature. The Coef has been tried with different values, and was chosen based on smoothly converging rate. The ideal temperature in the scheme is set to 43 °C in the treated tumor region, and a value ranging from 40 to 42 °C in the preheating zone.

The flow chart of adaptive scheme to reach ideal temperature in the treated region as well as the desired temperature in the preheating zone is shown in Fig. 2(a). The scheme is a finer-resolution optimization scheme as compared to lumped power deposition described in Huang et al. [3]. The conditional statement in the chart manages an important adaptive process for the heated tumor region. That is an evaluation criterion (Equations (4) and (5)), which shows that CV (n) (convergence value at iteration n) must be smaller than or equal to the designated convergence value (CV) to reach an optimal solution,

$$\text{CV}(n) = \frac{\sqrt{\dfrac{\sum_{\text{all target nodes}} (\Delta T(x,y,z))^2}{\text{total number of target nodes}}}}{(43-37)\,^\circ C}, \quad (4)$$

$$\text{CV}(n) \le \text{convergence value (CV)} \quad (5)$$

The target nodes in Equation (4) represent nodes in treated region, as well as nodes in preheating zone if the zone was employed. In that case, Equation (4) becomes,

$$\text{CV}(n) = \frac{\sqrt{\dfrac{\sum_{\text{all target nodes}} (\Delta T(x,y,z))^2 + (\Delta T_{\text{pre}}(x,y,z))^2}{\text{total number of target nodes}}}}{(43-37)\,^\circ C} \quad (6)$$

where $\Delta T_{\text{pre}}(x,y,z)$ is the difference between desired preheating zone temperature (T_{pre}) and calculated one as shown in Equation (7).

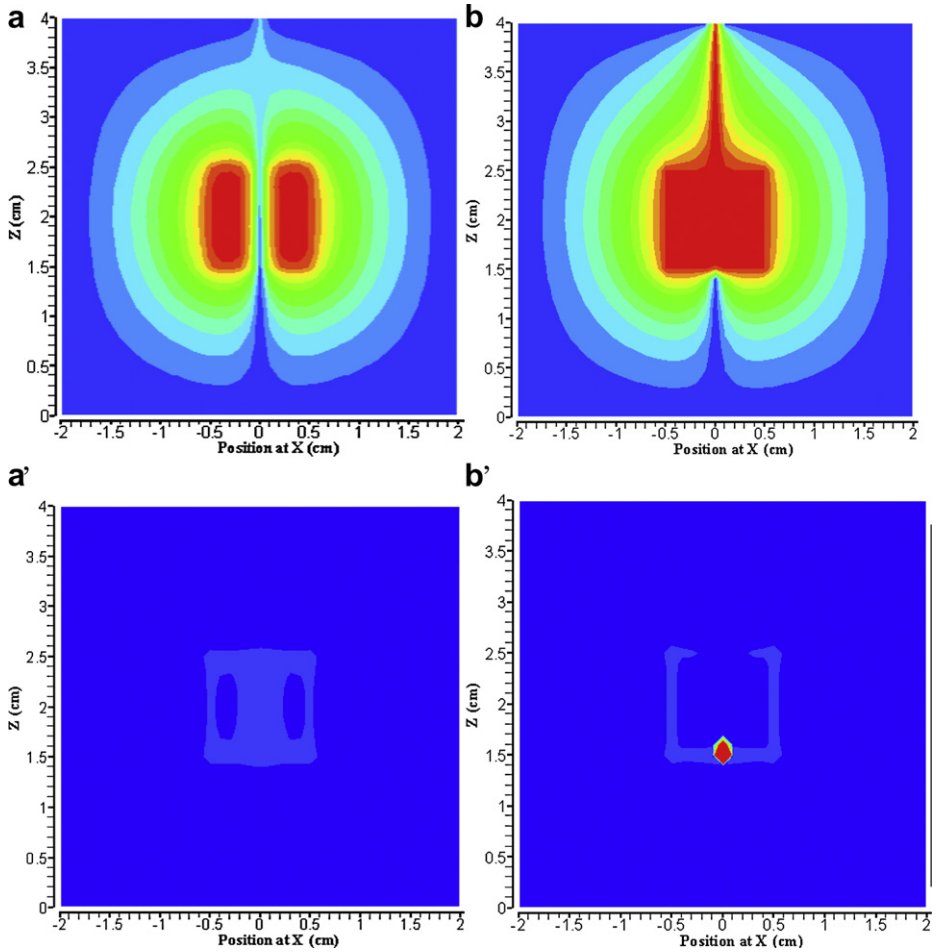

Fig. 3. The impact of convergence value on the optimized temperature and power density deposition distributions of the central X–Z plane. Temperature distributions are shown for a 0.8-mm diameter blood vessel with a blood velocity of 7.5 cm s^{-1} passing through the center of treated region at (a) CV = 10% and (b) CV = 1.25%. Their corresponding absorbed power density distributions are shown in (a′) and (b′), respectively. (unit in figure, Temperature: °C and Power Density: W m^{-3})

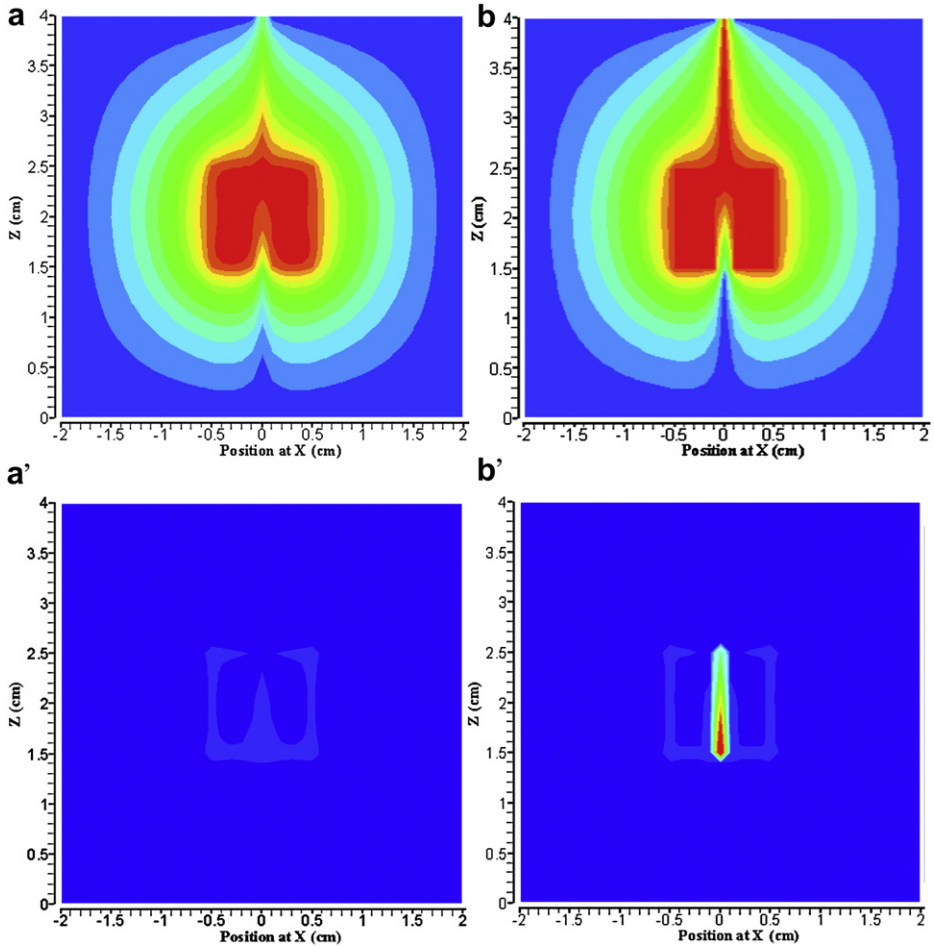

Fig. 4. The impact of blood vessel size on the optimized temperature and power density deposition distributions of the central X–Z plane. Temperature distributions are shown in (a) a 0.2-mm and (b) a 0.8-mm diameter blood vessel. Their corresponding absorbed power density distributions are shown in (a′) and (b′), respectively.

$$\Delta T_{\mathrm{pre}}(x,y,z) = T_{\mathrm{pre}} - T(x,y,z) \tag{7}$$

2.3. Preheating zone

The purpose of the preheating zone is to elevate blood temperature before blood entering the treated region in order to effectively reduce the cooling effect of blood on the treated region due to heat convection of blood vessel. The zone, as shown in Fig. 1(b), is adjacent to the tumor boundary and a parallelepiped with the two important parameters under investigation: preheating zone temperature (T_{pre}) and preheating length (L_{pre}). In addition to L_{pre} = 5-mm, we also studied L_{pre} = 8-mm to compare the effect of different preheating lengths. The preheating temperature, T_{pre}, ranging from 40 to 42 °C was considered in the study.

To reveal the preheating impacts on the temperature distribution of treated tumor region, a parameter "dtindex" is introduced to illustrate the difference between calculated and ideal temperatures in the treated volume during optimization process. It is defined as:

$$\mathrm{dtindex} = \frac{|T_{\mathrm{ideal}}(x,y,z) - T(x,y,z)|}{6.0} \tag{8}$$

and it is a function of space. Ideal temperature distribution in the treated volume is assumed to be 43 °C, uniform in space, in the present study. The divisor of 6 is chosen due to the increment of temperature from initial 37 °C to the ideal 43 °C. The value of "dtindex" is positive by absolute value and ranges from 0.0 to 1.0 in normal operations (i.e. gradual temperature increments toward ideal temperature). A value near 0.0 means the temperature approaches very close to ideal temperature and far away from the ideal temperature if near 1.0.

2.4. Mathematical and numerical modelings

Considering thermally significant blood vessel, both solid tissue and blood temperatures need to be calculated. Therefore, tissue field equation and convective blood vessel energy equation models are used to model the situation. The tissue temperature is described by Pennes bio-heat transfer equation. That is,

$$\nabla\cdot(k\nabla T(x,y,z)) - \dot{w}_{\mathrm{b}}c_{\mathrm{b}}(T(x,y,z) - T_{\mathrm{a}}) + P(x,y,z) = 0 \tag{9}$$

where k, c_{b}, $\dot{w}_{\mathrm{b}}$, and P are the thermal conductivity of soft tissue, specific heat of blood, blood perfusion rate and absorbed thermal power density which is a function of space, respectively. ∇ is the differential operator. Conduction occurs in all three directions in the tissue matrix, and the outer control volume surface is held at a constant reference temperature (i.e. identical to the inlet artery temperature).

The convective energy equation is solved for the blood vessel model. That is,

$$m_{\mathrm{b}}c_{\mathrm{b}}\nabla T_{\mathrm{b}}(x,y,z) = Nu\cdot k_{\mathrm{b}}\pi(T_{\mathrm{w}}(x,y,z) - T_{\mathrm{b}}(x,y,z)) + P(x,y,z)\pi R_{\mathrm{bv}}^2 \tag{10}$$

where m_{b} is the blood mass flow rate at vessel segment. Nu, k_{b}, R_{bv} and T_{w} are Nusselt number, thermal conductivity in blood,

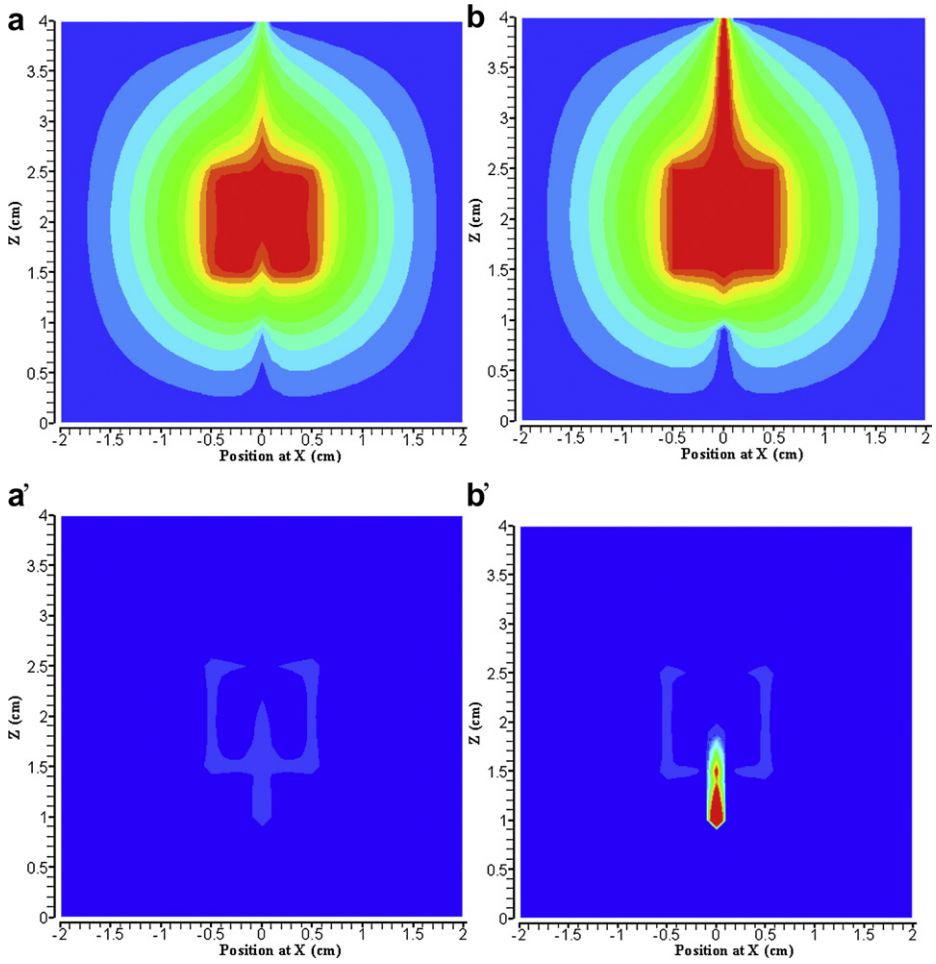

Fig. 5. The impact of preheating zone on the optimized temperature and power density distributions of the central *XZ* plane. The preheating zone is with L_{pre} = 5-mm and T_{pre} = 42 °C. Temperature distributions are shown in (a) a 0.2-mm and (b) a 0.8-mm diameter blood vessel. Their corresponding absorbed power density distributions are shown in (a′) and (b′), respectively.

radius of blood vessel and blood vessel wall temperature, respectively. We assumed the velocity profile of blood flow in vessel to be fully developed and uniform in cross section, since earlier studies showed the insignificant difference between a uniform and non-uniform velocity profiles [18,19]. The vessel heat transfer coefficient is calculated by using a constant Nusselt number of 4.0, which is considered reasonable for common blood vessels [6,7].

The numerical scheme used to calculate the temperatures is a black-and-red finite difference SOR method [7] with upwind differencing used for the vessels. The numerical details were described by Huang [7]. The property values used in treated tumorous and non-treated normal tissues are $k = k_b$ = 0.5 W m^{-1} °C^{-1}, $c = c_b$ = 4000 J kg^{-1} °C^{-1} and ρ = 1000 kg m^{-3}. In this study, a finite difference with nodal spacing of 1 mm was used. The boundary temperature is set to 37 °C at the outer control volume surfaces. Inlet temperature of vessel to the control volume is also set to 37 °C. The legends of temperature and power density distributions in 2-D contour plots throughout this paper with their corresponding units are shown in Fig. 2(b).

Table 2
Total absorbed power deposition comparisons in the treated tumor region and preheating zone, with and without the application of preheating zone (L_{pre} = 5-mm or 8-mm, and T_{pre} = 40, 41 or 42 °C), on several sizes (diameters from 0.2-mm to 1-mm) of thermally significant single blood vessels. The CV is 3.5% and numbers indicated inside the parenthesis are total power: tumor power: preheating zone power (Watt). The total absorbed power deposition was the sum of the tumor region power and the preheating zone power.

	Blood vessel diameter 1.0 mm	Blood vessel diameter 0.8 mm	Blood vessel diameter 0.6 mm	Blood vessel diameter 0.2 mm
Without preheat zone				
	(2.06:2.06:0.0)	(1.37:1.37:0.0)	(0.81:0.81:0.0)	(0.40:0.40:0.0)
With a 5-mm preheat zone at different preheat temperatures				
Preheat temperature 40 °C	(1.94:1.56:0.39)	(1.31:1.08:0.23)	(0.79:0.70:0.09)	(0.40:0.40:0.00)
Preheat temperature 41 °C	(2.04:1.49:0.55)	(1.36:1.04:0.32)	(0.81:0.68:0.14)	(0.40:0.39:0.01)
Preheat temperature 42 °C	(2.24:0.74:1.50)	(1.49:0.61:0.88)	(0.85:0.65:0.20)	(0.40:0.39:0.01)
With a 8-mm preheat zone at different preheat temperatures				
Preheat temperature 40 °C	(1.91:1.40:0.51)	(1.29:0.99:0.30)	(0.79:0.66:0.13)	(0.40:0.39:0.01)
Preheat temperature 41 °C	(2.05:1.31:0.74)	(1.37:0.94:0.44)	(0.82:0.63:0.19)	(0.40:0.39:0.01)
Preheat temperature 42 °C	(2.22:0.57:1.64)	(1.48:0.50:0.98)	(0.87:0.44:0.43)	(0.40:0.38:0.02)

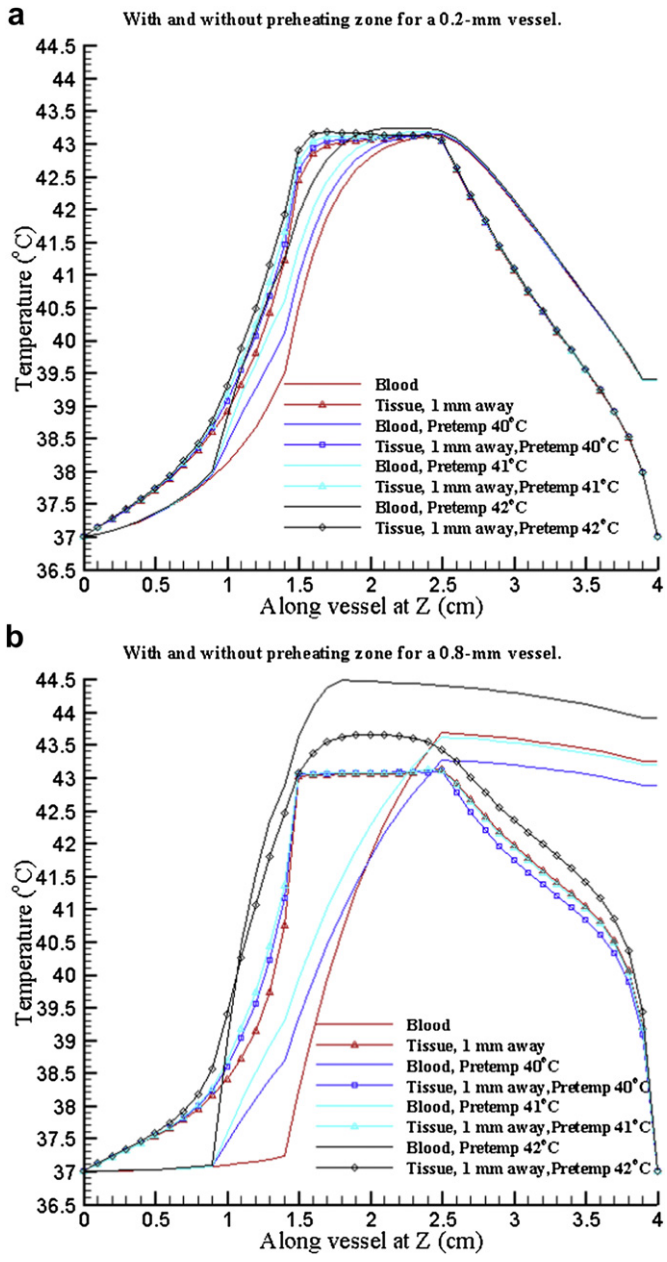

Fig. 6. The figure shows the blood and its surrounding tissue temperature (1-mm away from the center of vessel) distributions for (a) a 0.2-mm and (b) a 0.8-mm diameter blood vessel along blood flowing direction (Z) through the treated tumor region (1.5 cm $\leq Z \leq$ 2.5 cm) with and without a preheating zone. The preheating temperatures T_{pre} varies from 40 to 42 °C.

2.5. A vascular network model with vessels partially surrounding a treated tumor

A vascular network model presented by Huang et al. [3] is employed to evaluate the preheating strategy studied here. The model geometry is a parallelepiped of 8 cm by 8 cm by 8.2 cm. In the interior, sets of branching vessels in size hierarchy carry and collect blood within tissue. The model contained seven levels branching vessels in which diameters decrease between two consecutive vessel levels by a ratio from level 1 to level 7 (except level 6 to level 7). Namely, a large main artery blood vessel of level 1 carries blood to smaller artery vessels in gradual and branching manner (i.e. level 2, level 3… etc), as blood is brought into increasing number of smaller vessels. And, some of blood vessels partially surround the tumor and some smaller vessels penetrate into the treated tumor as described in the model [3]. The idea is to configure a preheating zone on the main blood vessel just before it enters the tumor region to realize the preheating zone's impacts on the treated tumor temperature distributions.

3. Results

3.1. Effect of convergence value (CV)

Fig. 3 shows the impact of convergent criterion on temperature and absorbed power density distributions without preheating blood vessels. The results show a 0.8-mm diameter blood vessel with blood velocity of 7.5 cm s^{-1} passing through the center of treated region; temperature distributions on the central X–Z plane, with CVs of 10% and 1.25% shown in Fig. 3(a) and (b), respectively. Their corresponding absorbed power density distributions are shown in Fig. 3(a′) and (b′). Ranges used in the figures are from 37 to 43 (°C) for temperature, and from 10^5 to 10^8 (W m^{-3}) for absorbed power density as shown in Fig. 2(b). We use them consistently throughout all figures in the current study unless notified.

At CV = 10%, power deposition is added up gradually on the treated region, raising temperatures from initial blood and tissue boundary conditions of 37 °C. Apparently, tumor tissue temperatures are higher than blood temperatures. Absorbed power is focused at the tumor boundary and the internal vessel–tissue interface.

At CV = 1.25%, uniform ideal temperature of 43 °C is reached in treated region but with a "tail" of high temperature blood region. An extreme power density is located at the pointed spot of vessel entering to the treated tumor and it is close to 10^3 times the absorbed power density on tumor boundary. Although a small CV helps to illustrate results in more details, it takes excessive computational time to execute iterative scheme.

3.2. Heating difficulty of thermally significant blood vessel without preheating zone

Fig. 4(a) and (b) shows optimized temperature distributions for a 0.2-mm and a 0.8-mm diameter blood vessel, respectively, with a CV of 3.5%, and the corresponding power density distributions are shown in Fig. 4(a′) and (b′). For the case with a 0.2-mm vessel, the tail is much smaller than that in the 0.8-mm vessel, since a larger vessel carries a greater amount of blood flow with a lower temperature penetrating deeper into the tumor region. This causes the scheme to focus more power at the entrance of blood and along the vessel path. As it can be seen, significant difference in power depositions between blood vessel and tumor boundary. Unless notified, the CVs for the following figures are set to 3.5%.

3.3. Effect of the implementation of preheating zone

Fig. 5 shows how a preheating zone impacts on optimized temperature and power density distributions on the central XZ plane. The preheating zone is with L_{pre} = 5-mm and T_{pre} = 42 °C. The optimized temperature distributions for a 0.2-mm diameter blood vessel and a 0.8-mm vessel are shown in Fig. 5(a) and (b), respectively. Their corresponding power density distributions are shown in Fig. 5(a′) and (b′). With implementation of the preheating zone, the power deposition in tumor region was significantly reduced.

3.4. Effects of preheating zone length (L_{pre}) and temperature (T_{pre})

Table 2 shows absorbed power deposition comparisons in the treated tumor region and preheating zone, with and without the application of preheating zone for L_{pre} = 5-mm or 8-mm, and T_{pre} = 40, 41 or 42 °C, on several sizes (diameters from 0.2-mm to 1-mm) of thermally significant single blood vessels. Numbers indicated inside the parenthesis are total power: tumor power: preheating power (Watt). The total absorbed power is the sum of the tumor power and the preheating power.

Regardless of vessel sizes, there is more power deposited on an 8-mm preheating zone than a 5-mm one. This causes the decrease of absorbed power in the tumor region as indicated in Table 2. However, total absorbed power is decreased only at the lowest T_{pre} (i.e., 40 °C) for large vessel sizes (0.8-mm and 1.0-mm).

Fig. 6 shows the blood and its surrounding tissue temperatures along blood flowing direction (z) through treated tumor region (1.5 cm $\leq z \leq$ 2.5 cm) with and without the preheating zone at different T_{pre} (from 40 to 42 °C) for 0.2-mm and 0.8-mm blood vessels. The figures shows four sets of data and they are: without preheating zone, with T_{pre} = 40 °C, T_{pre} = 41 °C and T_{pre} = 42 °C. Each set contains blood temperatures and tissue temperatures (1-mm away from the center of vessel) along Z direction and is shown in the same color (in the web version) in both Fig. 6(a) and (b). Additional symbol for distinction was added in the lines for tissue temperatures.

For the 0.8-mm vessel shown in Fig. 6(b), blood temperature is elevated to 43 °C with rather steep gradient. The high thermal gradient makes blood either moving along vessel with some penetrating distance before reaching 43 °C in the tumor region, or shooting over 43 °C before entering the region when preheating temperature is 42 °C.

3.5. Comparison of power deposition in treated tumor region and preheating zone

Fig. 7 shows the comparison of optimized total, tumor and preheating power depositions, with and without the application of preheating zone L_{pre} (5-mm or 8-mm) and different T_{pre} (from 40 to 42 °C), for thermally significant blood vessels (0.2-mm and 0.8-mm) during hyperthermia treatment. The notation "5 mm-40" stands for a 5-mm preheating zone length and a preheating temperature of 40 °C. As preheating power increases, tumor power decreases. It appears very clear for the 0.8-mm vessel. For the 0.2-mm vessel, much less total power is required to heat the tumor region and its preheating power is negligible. Furthermore, the other impact of preheating on the treated region is the reduction of significant cooling spots in the treated region. Fig. 8 shows dtindex distributions on the central x–z plane (with the thermally significant blood vessel) to reveal preheating impacts on the treated tumor temperatures for the cases shown in Fig. 7(b). For cases presented on the

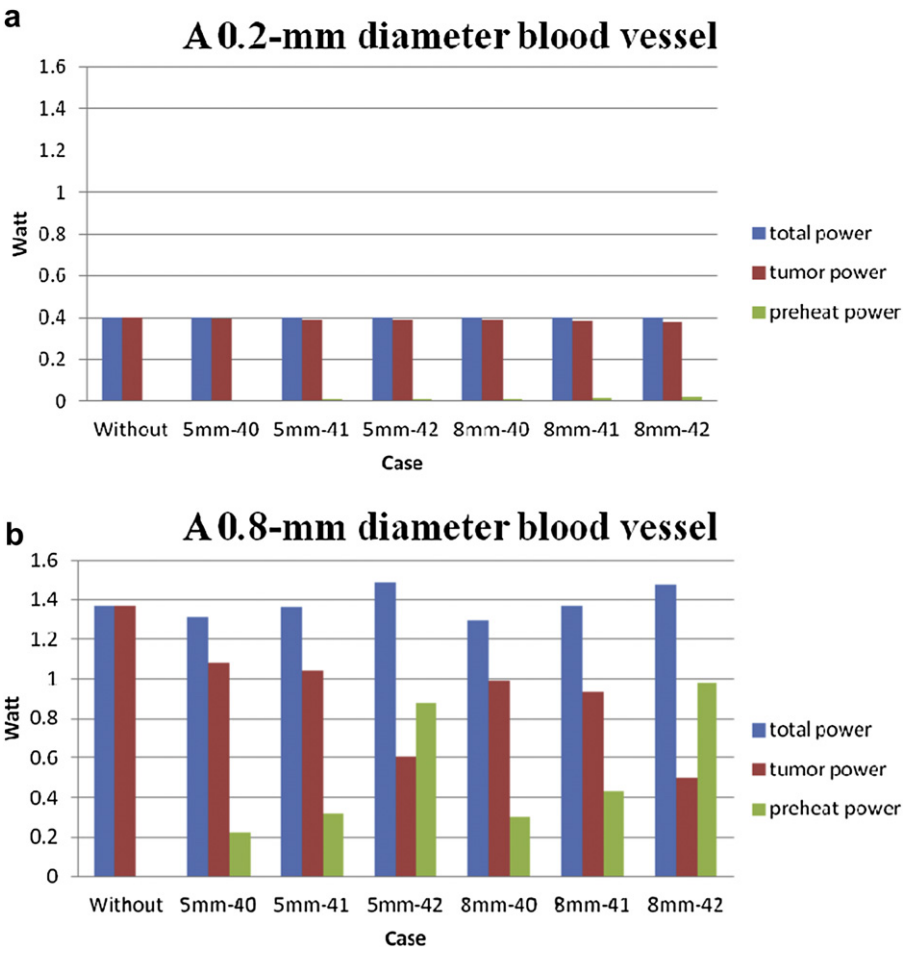

Fig. 7. Comparisons of optimized total, tumor and preheating absorbed power depositions, with and without the application of preheating zone. Preheating length L_{pre} = 5-mm or 8-mm and different preheating temperatures T_{pre} are used for (a) a 0.2-mm and (b) a 0.8-mm diameter blood vessel during hyperthermia treatment. (notation "5 mm-40" stands for a 5-mm preheating zone length and a preheating temperature of 40 °C)

sub-figures, they are: (a) without preheating zone, (b) 5 mm-40, (c) 5 mm-41, (d) 5 mm-42, (e) 8 mm-40, (f) 8 mm-41, (g) 8 mm-42 and (h) dtindex ranging from 0.1 to 0.7. Significant cooling spot in red is shown in Fig. 8(a) (the case without preheating treatment), which has been damped when treatments conducted with preheating zone for cases in Fig. 8(b)–(g). Fig. 8(h) indicates that red color (in the web version) in the contour plots means dtindex value approaching 0.7 and significant cooling effect.

4. Discussions

4.1. Elevation of blood temperature at the entrance of treated region

As maintaining the uniform temperature during hyperthermia treatment, Figs. 4 and 5 point out the difficulty in overcoming the cooling effect of thermally significant blood vessels in the entrance of treated region. To understand the impacts of preheating zone, we compared the blood temperature at 1-mm in front of the vessel entrance into the treated region. Fig. 6 shows that for the 0.2-mm vessel case without the preheating zone, the blood temperature at $Z = 14$ mm is 39.49 °C. With the implementation of preheating zone, L_{pre} = 5-mm, and T_{pre} = 40, 41 and 42 °C, the blood temperature at that location becomes 40.09, 40.60 and 41.23 °C; They are 0.60, 1.11 and 1.74 °C increases, respectively. For the larger blood vessel case (0.8-mm), without the preheating zone, the entrance blood temperature is 37.23 °C. With the implementation of preheating zone, L_{pre} = 5-mm, and T_{pre} = 40, 41 and 42 °C, the entrance blood temperature becomes 38.69, 39.30 and 42.88 °C; They are 1.46, 2.07 and 5.65 °C increases, respectively. As to L_{pre} = 8-mm, for the 0.8-mm blood vessel case, at T_{pre} = 40, 41 and 42 °C, the blood temperature is 39.16, 40.02 and 43.45 °C, respectively. An increase of preheating zone length suggests a little more elevation of blood temperature can be obtained. The results suggest that the preheating zone is able to elevate the blood temperature before entering into the treated region. However, the notable increase of 5.65 °C for the 0.8-mm vessel case at T_{pre} = 42 °C and L_{pre} = 5-mm is due to the adaptive optimization scheme and strong convective heat transport.

4.2. Significant decrease of tumor power caused by preheating zone

By preheating thermally significant blood vessel, the thermal energy which is required to heat the treated tumor is significantly reduced as shown in Table 2. For the 1.0-mm vessel case with L_{pre} = 5-mm and T_{pre} = 40 °C, it is near 25% decrease of tumor power as compared to that of the case without the preheating zone. At T_{pre} = 41 °C and 42 °C, the decrease of tumor power becomes 28% and 64%, respectively. On the smaller vessel case, 0.2-mm for example, with L_{pre} = 5-mm, and T_{pre} = 40 °C, 41 °C and 42 °C, the decrease of tumor power is approximately 1%, 2% and 3%, respectively. The results indicate that larger blood vessels, implication of larger blood flow, significantly impact thermal energy deposition on the treated region. On the other hand, smaller blood vessels have minor or negligible impact on the treated region due to their thermal entrance lengths are short and able to reach thermal equilibrium fast.

4.3. Importance of CV in the presence of blood vessel within the treated region

In order to maintain a uniform target temperature in treated tumor having a thermally significant vessel, optimization requires

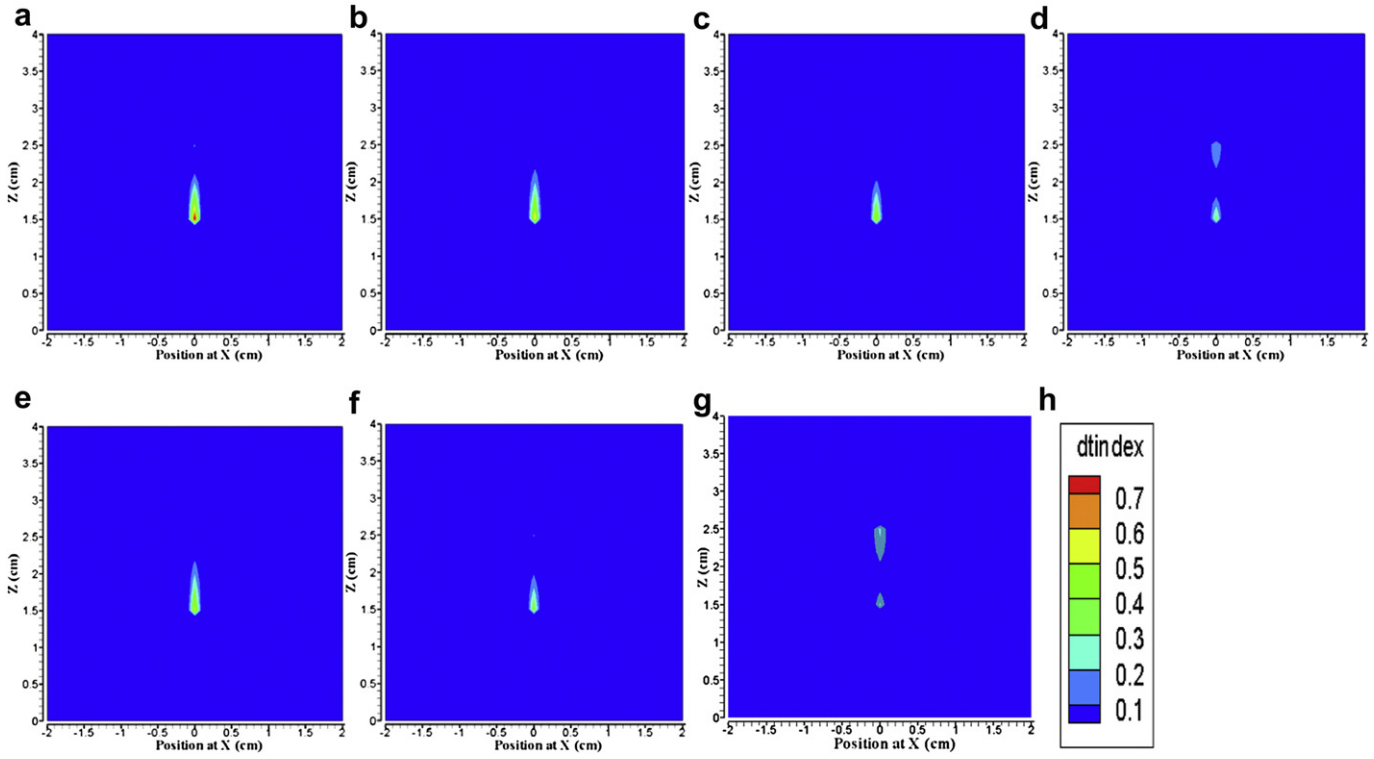

Fig. 8. dtindex distributions on the central X–Z plane (with a thermally significant blood vessel) to reveal the impact of preheating on the treated tumor temperatures for the cases shown in Fig. 7(b). For cases presented on the sub-figures, they are (a) without preheating zone (b) 5 mm-40 (c) 5 mm-41 (d) 5 mm-42 (e) 8 mm-40 (f) 8 mm-41 (g) 8 mm-42 and (h) dtindex ranging from 0.1 to 0.7 (notation "5 mm-40" stands for a 5-mm preheating zone with a preheating temperature of 40 °C).

a small CV and it produces extreme power deposition on the vessel. Moreover, a small CV helps to illustrate the cooling effect of the vessel near tumor boundary as shown in Fig. 3. For CV equal to 1.25%, Fig. 9 shows the blood and its surrounding tissue temperatures along blood flowing direction through treated tumor region (1.5 cm $\leq z \leq$ 2.5 cm) with and without the application of preheating zone. Significant changes exist in blood temperatures in the front and to the rear of the treated region, particularly for a large blood vessel. Tissue temperatures remain close to 43 °C in the treated region and their variations are within 0.5 °C as compared to Fig. 6. Thus, a smaller CV value made significant contributions to the tendency of blood and tissue temperature distributions. Results of the smaller CV value reveal that high thermal gradients play a decisive role in the presence of blood vessels during the optimization hyperthermia process.

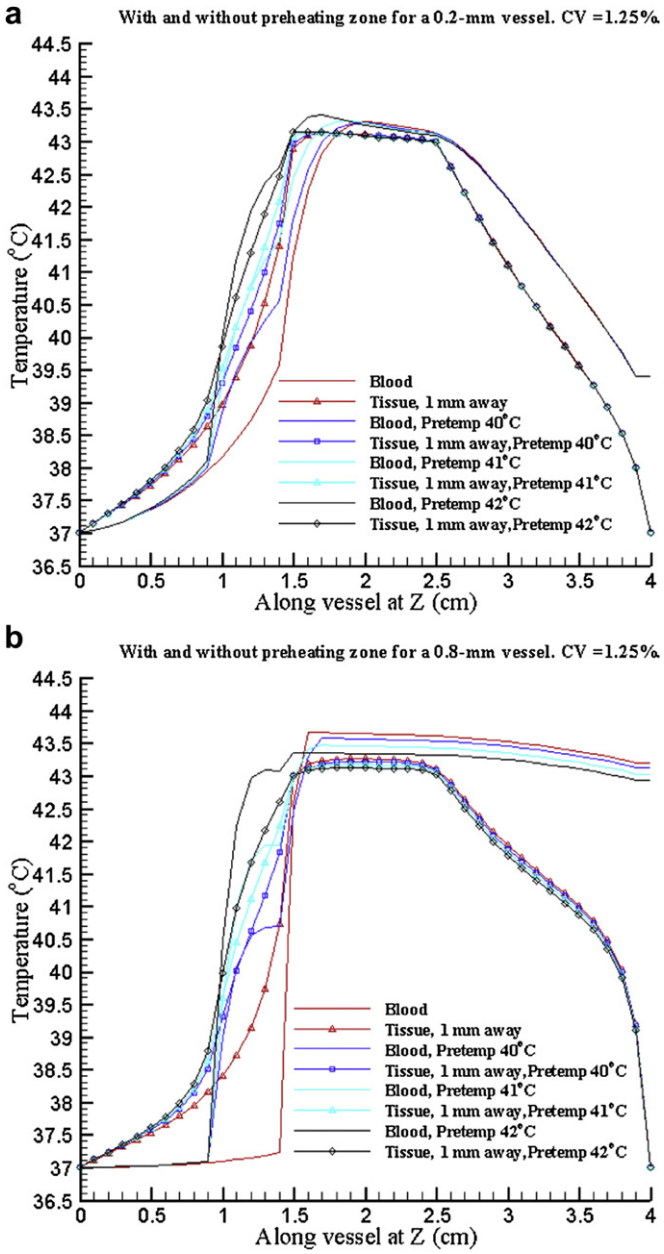

Fig. 9. The figure shows the blood and its surrounding tissue temperature (1-mm away from the center of vessel) distributions for (a) a 0.2-mm and (b) a 0.8-mm diameter blood vessel along blood flowing direction (Z) through treated tumor region (1.5 cm $\leq Z \leq$ 2.5 cm) with and without a preheating zone. The CV is 1.25%.

4.4. Preheating strategy applied to a vascular network model

Furthermore, we applied the preheating strategy to a vascular network model [3]. The preheating zone was placed on the main vessel (i.e. level 1, 1-mm diameter vessel) which partially surrounded the treated tumor: a cube of 2 cm by 2 cm by 2 cm. The control volume is a parallelepiped of 8 cm by 8 cm by 8.2 cm. Details are described in reference [3]. Fig. 10 shows temperature distributions on the y–z plane facing the front treated tumor boundary (at x = 4.2 cm) of 2 cm by 2 cm in dimensions, located from y = 0.02 m to 0.04 m and z = 0.04 m to 0.06 m. Fig. 10(a) without preheating and Fig. 10(b) with preheating (L_{pre} = 8 mm and T_{pre} = 42 °C) are compared here. The preheating zone is placed on level 1 vessel (Different level sizes of blood vessels are highlighted

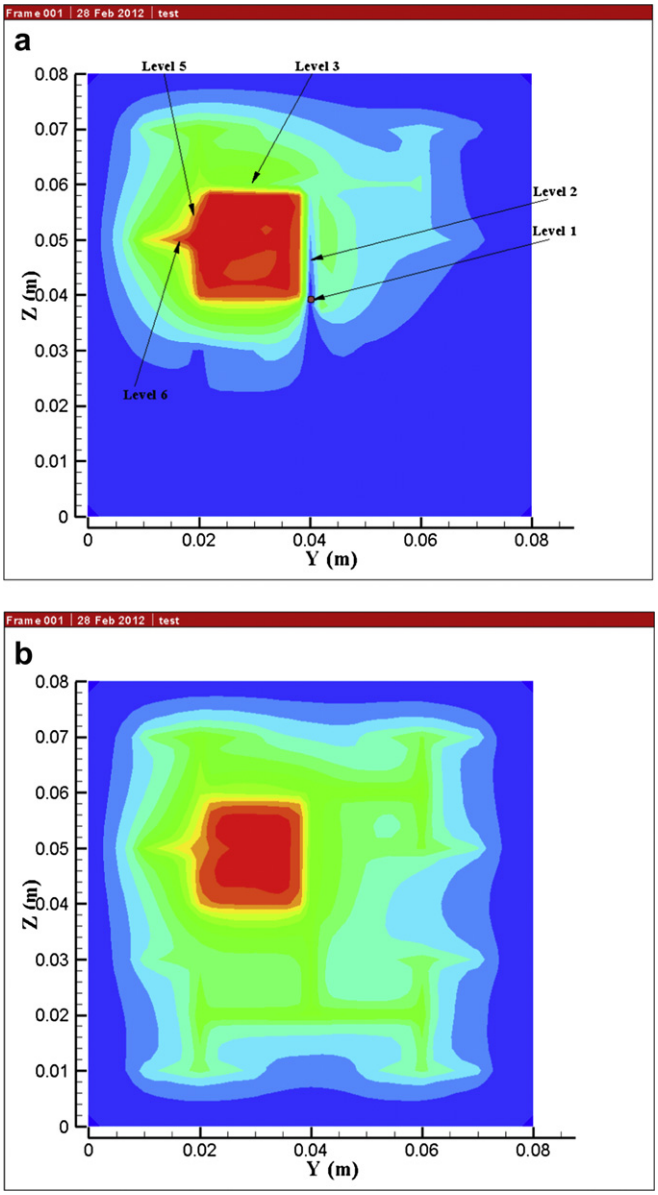

Fig. 10. The impact of preheating strategy on temperature distributions in a vascular network model [3]. The figure shows (a) without preheating and (b) with preheating (L_{pre} = 8 mm and T_{pre} = 42 °C) on Level 1 main vessel partially surrounding the tumor. (Different level sizes of blood vessels were marked around the treated tumor in Fig. 10(a): Level 1: running in perpendicular to the plane (positive X-axis), Level 2: running up in positive Z-axis, Level 3: running in Y-axis, Level 5: running down in Z-axis and Level 6: running in Y-axis)

in Fig. 10(a) around the treated tumor and its boundaries: Level 1: running in perpendicular to plane (positive *X*-axis), Level 2: running up in positive *Z*-axis, Level 3: running in *Y*-axis, Level 5: running down in *Z*-axis and Level 6: running in *Y*-axis).

Blood vessels are running in different directions but partially surrounding the treated tumor (or branching smaller vessels into the tumor). Preheating the upstream zone (adjacent to the treated tumor) at level 1 artery with $L_{pre} = 8$ mm and $T_{pre} = 42\ ^{\circ}C$ causes rather high temperatures along blood paths as well as tumor surrounding (Fig. 10(b)). It shows less power required to heat up vessels around tumor as well as both interior tumor tissue and smaller branching vessels as shown in Fig. 10. Smooth and homogenous temperatures in treated tumor volume can be achieved with preheating.

5. Conclusion

Cooling effects by blood flow during hyperthermia treatments can be significantly improved if a preheating zone is placed on the blood vessel adjacent to treated tumor region and the blood before entering the tumor is heated. Higher preheating temperature and longer preheating zone are helpful to elevate blood temperature before blood entering the treated region, especially for a large blood vessel. The preheating could prevent extreme power deposition in the tumor region as well.

We have proposed the preheating strategy using a single blood vessel tumor model as well as a countercurrent vascular network model (7-level vessels) [3,7]. Smooth and homogenous temperatures in treated tumor volume could be achieved with preheating. Furthermore, for a better homogeneous temperature distribution in the treated region, modification of adaptive optimization scheme is required [20]. The inclusion of thermally significant blood vessels in the treated tumor region created abrupt thermal resistances at vessel paths. Separate absorbed power density for heating blood and solid tissue is recommended during optimization.

Acknowledgements

The authors would like to thank the National Science Council of Taiwan for partially supporting this research under no. NSC 100-2221-E-032 -013.

References

[1] P.W. Vaupel, D.K. Kelleher, Pathophysiological and vascular characteristics of tumours and their importance for hyperthermia: heterogeneity is the key issue, Int. J. Hyperth. 26 (3) (2010) 211–223.
[2] M.D. Hurwitz, Today's thermal therapy: not your father's hyperthermia: challenges and opportunities in application of hyperthermia for the 21st century cancer patient, Am. J. Clin. Oncol. 33 (1) (2010) 96–100.
[3] H.W. Huang, C.T. Liauh, T.C. Shih, T.L. Horng, W.L. Lin, Significance of blood vessels in optimization of absorbed power and temperature distributions during hyperthermia, Int. J. Heat Mass Transfer 53 (2010) 5651–5662.
[4] H.H. Pennes, Analysis of tissue and arterial blood temperature in the resting human forearm, J. Appl. Phys. 1 (1948) 93–122.
[5] M.M. Chen, K.R. Holmes, Microvascular contributions in tissue heat transfer, Ann. N.Y. Acad. Sci. 335 (1980) 137–150.
[6] J.C. Chato, Heat transfer to blood vessels, ASME J. Biomech. Eng. 110 (1980) 110–118.
[7] H.W. Huang, Simulation of large vessels in hyperthermia therapy, M.S. thesis. University of Arizona, Tucson, AZ, 1992.
[8] H.W. Huang, C.L. Chan, R.B. Roemer, Analytical solutions of Pennes bio-heat transfer equation with a blood vessel, ASME J. Biomech. Eng. 116 (1994) 208–212.
[9] J.W. Baish, Heat transport by counter current blood vessels in the presence of an arbitrary temperature gradient, ASME J. Biomech. Eng. 112 (1990) 207–211.
[10] J. Crezee, J.J.W. Lagendijk, Experimental verification of bio-heat transfer theories: measurement of temperature profiles around large artificial vessels in perfused tissues, Phys. Med. Biol. 35 (1990) 905–923.
[11] J. Crezee, J.J.W. Lagendijk, Temperature uniformity during hyperthermia: the impact of large vessels, Phys. Med. Biol. 37 (1992) 1321–1337.
[12] R. Rawnsley, R.B. Roemer, A. Dutton, The simulation of large vessel effects in experimental hyperthermia, ASME J. Biomech. Eng. 116 (1994) 256–262.
[13] M.C. Kolios, M.D. Sherar, J.W. Hunt, Blood flow cooling and ultrasonic lesion formation, Med. Phys. 23 (7) (1996) 1287–1298.
[14] W.L. Lin, T.C. Liang, J.Y. Yen, H.L. Liu, Y.Y. Chen, Optimization of power deposition and a heating strategy for external ultrasound thermal therapy, Med. Phys. 28 (10) (2001) 2172–2181.
[15] H.S. Tharp, R.B. Roemer, Optimal power deposition with finite-sized, planar hyperthermia applicator arrays, IEEE Trans. Biomed. Eng. 39 (6) (1992) 569–579.
[16] J.J.W. Lagendijk, The influence of blood flow in large vessels on the temperature distribution hyperthermia, Phys. Med. Biol. 27 (1982) 17–23.
[17] R.B. Roemer, Optimal power deposition in hyperthermia. I. The treatment goal: the ideal temperature distribution: the role of large blood vessels, Int. J. Hyperth. 7 (2) (1991) 317–341.
[18] T.-L. Horng, W.-L. Lin, C.-T. Liauh, T.-C. Shih, Effects of pulsatile blood flow in large vessels on thermal dose distribution during thermal therapy, Med. Phys. 34 (4) (2007) 1312–1320.
[19] T.-C. Shih, T.-L. Horng, H.-W. Huang, K.-C. Ju, T.-C. Huang, P.-Y. Chen, Y.-J. Ho, W.-L. Lin, Numerical analysis of coupled effects of pulsatile blood flow and thermal relaxation time during thermal therapy, Int. J. Heat Mass Transfer 55 (2012) 3763–3773.
[20] H.-W. Huang, C.-T. Liauh, C.-Y. Chou, T.-C. Shih, W.-L. Lin, A fast adaptive power scheme based on temperature distribution and convergence value for optimal hyperthermia treatment, Appl. Therm. Eng. 37 (2012) 103–111.